Gas Hydrate Phase Equilibrium in Porous Media: Mathematical Modeling and Correlation

ARTICLE *in* INDUSTRIAL & ENGINEERING CHEMISTRY RESEARCH · JANUARY 2012

Impact Factor: 2.59 · DOI: 10.1021/ie201904r

I&EC research
Industrial & Engineering Chemistry Research

ARTICLE

pubs.acs.org/IECR

Gas Hydrate Phase Equilibrium in Porous Media: Mathematical Modeling and Correlation

Amir H. Mohammadi,*[,†,‡] Ali Eslamimanesh,[†] and Dominique Richon[†,‡]

[†]MINES ParisTech, CEP/TEP—Centre Énergétique et Procédés, 35 Rue Saint Honoré, 77305 Fontainebleau, France

[‡]Thermodynamics Research Unit, School of Chemical Engineering, University of KwaZulu-Natal, Howard College Campus, King George V Avenue, Durban 4041, South Africa

Farhad Gharagheizi

Department of Chemical Engineering, Buinzahra Branch, Islamic Azad University, Buinzahra, Iran

Mohammad Yazdizadeh

School of Chemical and Petroleum Engineering, Shiraz University, 71348-51154 Shiraz, Iran

Jafar Javanmardi, Hamed Hashemi, Mojdeh Zarifi, and Saeedeh Babaee

Department of Chemical Engineering, Shiraz University of Technology, 71555-313 Shiraz, Iran

Supporting Information

ABSTRACT: In this paper, we present two different approaches to represent/predict the gas hydrate phase equilibria for the carbon dioxide, methane, or ethane + pure water system in the presence of various types of porous media with different pore sizes. The studied porous media include silica gel, mesoporous silica, and porous silica glass. First, a correlation is presented, which estimates the hydrate suppression temperature due to the pore effects from the ice point depression (IPD). In the second place, several mathematical models are proposed using the least squares support vector machine (LSSVM) algorithm for the determination of the dissociation pressures of the corresponding systems. The results indicate that although the applied correlation based on the (IPD) leads to obtaining reliable results for the gas hydrate systems in the presence of porous silica glass media, the developed LSSVM models seem to be more general due to their predictive capability over all of the investigated systems.

1. INTRODUCTION

Since the last century, it has been argued that there are huge amounts of natural gas hydrates in the sediments under the seafloor (subsea sediments) and the permafrost zone (cryotic soil) in both on-shore and off-shore buried areas.[1,2] Meticulous theoretical and experimental investigations along with comprehensive field studies have demonstrated that the aforementioned masses of gas hydrates are normally dispersed in pores of porous media such as clay, silt, sand, and muds.[2−4] The natural gas hydrates reserves (mostly contain methane) can be considered as future energy resources. At the present time, these reserves are not generally used; however, their probable leaks have great potential for increasing the emission of greenhouse gases to the atmosphere.[1−8] Moreover, in natural gas/oil production processes, the existing/formation of gas hydrates in porous media, structured by different kinds of sandstones, merit careful consideration.

However, unlike gas (clathrate) hydrate formation in bulk phases (including hydrate formation from water, powdered ice, and water content of gases), capillary forces such as surface or interfacial tension play an important role in the formation of clathrate hydrates in porous media. It is generally believed that these interfacial forces lead to inhibition effects on clathrate hydrate formation in pores.[1−5] Consequently, the phase boundary of corresponding gas hydrate formation shifts to present more stable hydrate conditions at lower temperature/higher pressure conditions.[1−6] There are not many experimental data regarding the phase equilibria of clathrate hydrates in non-artificial porous media reported in open literature,[4] due to the fact that these measurements are not normally an easy task.[1−9] Perhaps, these studies have been begun by Handa and Stupin,[9] who investigated the hydrate formation in mesoporous media (silica gel pores).[1−7]

As well-established in numerous studies, thermodynamic models for prediction/representation of gas hydrate phase equilibria are generally based on the solid solution theory of van der Waals− Platteeuw[10] (vdW-P).[1−6,11−14] However, for prediction of the dissociation conditions of clathrate hydrates in porous media, the effects of capillary forces have to be

Received: August 25, 2011
Accepted: December 5, 2011
Revised: November 18, 2011
Published: December 05, 2011

Table 1. Experimental Hydrate Dissociation Conditions Applied to Develop/Check the Models

hydrate former	media	pore diameter (nm)	temp range (K)	pressure range (MPa)	ref
CH_4	silica gel porous	7	263−276.2	2.64−5.25	9
CH_4	silica gel porous	6.8, 14.6, 30.5	275.3−284.53	4.012−10.285	47
CH_4	silica gel porous	2, 3, 5, 7.5	244−276	1.6−4.26	48
CH_4	mesoporous silica	9.2, 15.8, 30.6	271.8−287.5	3.689−14.065	5
CH_4	mesoporous silica	9.2, 15.8, 30.6	271.8−287.5	3.689−14.065	52
CH_4	porous glass	10, 30, 50	277.2−283.7	4.8−8.5	53
CH_4	porous glass	15	266.15	2.2	54
CH_4	porous glass	9.2, 15.8, 30.6	271.8, 287.5	3.689−14.065	55
CO_2	silica gel porous	6.8, 14.6, 30.5	271.8−281.35	1.13−3.918	47
CO_2	silica gel porous	3, 5, 7.5	253−276	0.599−17.16	49
CO_2	porous glass	15	263.15−276.15	0.7−1.68	54
CO_2	porous glass	9.2, 15.8, 30.6	270.2, 279.8	1.407−3.33	55
C_2H_6	silica gel pores	6, 10, 15	243.15−277.15	0.112−1.504	50
C_2H_6	silica gel porous	6.8, 14.6, 30.5, 94.5	271.97−285.24	0.903−2.814	47

taken into account. Most of the corresponding models in the literature apply the Gibbs−Thomson relationship[3,9] for this purpose. In 1999, Clarke et al.[15] successfully presented a thermodynamic model for predicting hydrate dissociation conditions in the porous media taking into account the effect of capillary pressure and geometry of the pore sizes on activity of water. Later, almost the same procedure was pursued by Wilder et al.[16] A modification of these two models was proposed by Llamedo and co-workers[5] based on derivation of a more exact equation to evaluate hydrate−liquid interfacial tension.

Klauda and Sandler[17] extended their previously presented clathrate hydrate fugacity model[18] to gas hydrate formation in porous media implementing both surface energy and pore size distribution to account for the type of the investigated soil. They reported acceptable agreement of their model results in comparison with the existing experimental gas hydrate dissociation values. These two researchers later modified their model to use the sediment type, geothermal gradient, and seafloor depths as inputs and reported the maximum depth of hydrate stability for data collected in the Ocean Drilling Program as the predicted values (outputs).[19] Several authors have followed similar thermodynamic fugacity approaches.[3,20,21] More recently, Chen et al.[2] applied the Chen and Guo[22,23] two step gas hydrate formation mechanism to develop a thermodynamic model for prediction of the hydrate−water−gas equilibria in micropores for the hydrate formers including the mixtures of methane, ethane, and propane. Another approach has been pursued by Momeni et al.,[24] in which the capabilities of the artificial neural networks (ANNs) have been checked to predict the methane and ethane hydrate dissociation conditions in different porous media.

On the basis of the preceding explanations, there is still need to generate more accurate or simple models for representation/prediction of clathrate hydrates dissociation conditions in different porous media and various hydrate formers. In this work, we present a theoretically correct correlation and several mathematical models for evaluation of clathrate hydrates phase equilibria of the methane, carbon dioxide, or ethane systems in the presence of different porous media.

2. CORRELATION

Najibi et al.[25] proposed a correlation to relate the normal ice point depression (IPD) of aqueous solution due to the presence of thermodynamic inhibitors (salts and/or organic inhibitors) to gas hydrate suppression temperature of fluids in the presence of the same inhibitor aqueous solutions.[25,26] For this purpose, the following expression was developed[25,26]

$$\Delta T_{\text{hydrate}} = 0.683 \times \Delta T_{\text{ice}} \tag{1}$$

where $\Delta T_{\text{hydrate}}$ is the clathrate hydrate suppression temperature and ΔT_{ice} stands for the IPD. Application of eq 1 contributes to acceptable results for classical gas hydrate inhibitors.[25]

As already mentioned, the Gibbs−Thomson (Kelvin) equation is generally employed to evaluate the pore dissociation transition temperature depression (ΔT_{pore}) from the bulk transition temperature (T_{pore}):[3,9]

$$\frac{\Delta T_{\text{pore}}}{T_{\text{bulk}}} = \frac{-2\gamma' \cos\theta}{\rho \Delta H d} \tag{2}$$

where ΔT_{pore}, T_{bulk}, γ', ρ, ΔH, and d are the clathrate hydrate dissociation temperature depression in pores, clathrate hydrate dissociation temperature at bulk conditions, specific surface energy of the hydrate−liquid interface, the clathrate hydrate or gas-saturated liquid density, latent heat of hydrate dissociation, and pore diameter, respectively, and cos θ denotes the contact angle between the solid and the pore wall.

In this work, we extend Najibi et al.'s[25] correlation to predict the clathrate hydrate suppression temperature due to the pore effects from the IPD. Therefore, the following expression can be written:[26]

$$T_{\text{hydrate, pore}} = T_{\text{hydrate, bulk}} - 0.683 \times \Delta T_{\text{ice, pore}} \tag{3}$$

Equation 3 reveals that the hydrate dissociation temperature of a fluid at porous media condition ($T_{\text{hydrate,pore}}$) is related to the IPD ($\Delta T_{\text{ice,pore}}$) data (with respect to ice point at bulk condition, i.e., 273.15 K) and the clathrate hydrate dissociation temperature of the same fluid at bulk condition ($T_{\text{hydrate,bulk}}$). To apply the proposed correlation, a suitable thermodynamic predictive tool can be used to calculate the clathrate hydrate dissociation temperature of the same fluid system at bulk conditions.

dx.doi.org/10.1021/ie201904r |Ind. Eng. Chem. Res. 2012, 51, 1062–1072

3. MATHEMATICAL MODELING

3.1. Introduction to Support Vector Machine (SVM). To present the mathematical models, we look for appropriate relationships between the available experimental information considered as inputs of the models (temperature and pore size) and the desired output (hydrate dissociation pressure). For this purpose, powerful mathematical tools are required.

It has been discussed that the ANN-based models are generally capable of providing acceptable accuracy for different problems.[27−38] However, they have been shown to have possibilities of facing the random initialization of the networks and/or variation of the stopping criteria during optimization of the model parameters.[39−43] Another element to consider is that the ANN is a mathematical tool that users must be very careful to apply its subsequent results within the frame of the hypotheses and within the field of the data that allows determination of the parameters.[44] These factors may eventually make the researchers/engineers not to be confident about employing the ANN models for external predictions (i.e. inputs excluding those applied in training, optimization, and test procedures of treatment of the corresponding networks). Therefore, any extrapolation may not be recommended.

The SVM is considered to be a reliable and powerful algorithm organized from the machine-learning community.[39−43,45,46] Some of the advantages of the SVM-based methods over the traditional methods based on the ANNs are as follows:[39−43,45,46]

1. More probability for convergence to the global optimum;
2. Normally find a solution that can be quickly obtained by a standard algorithm;
3. No need to determine the network topology in advance, which can be automatically determined as the training process ends;
4. Generally less probability for the SVM[39] strategy to encounter overfitting problem;
5. No requirements for choosing the number of hidden nodes;
6. Acceptable generalization performance;
7. Fewer adjustable parameters;
8. Following convex optimization procedures.

The SVM[39] outstanding performance for solving static function approximation problems leads it to be perhaps more capable than the traditional empirical risk minimization principles. Additionally, because of their specific formulation, sparse solutions can be found, and both linear and nonlinear regressions can be employed for solving the corresponding problems.[39−43,45,46]

In 1999, Suykens and Vandewalle[40] introduced a modification to facilitate the solution of the original SVM algorithm[39] set of nonlinear equations (quadratic programming). The developed least-squares SVM (LSSVM)[40] encompasses the advantages similar to those of SVM,[39] although it requires solving a set of only linear equations (linear programming), which is much easier and more rapid as compared with the traditional SVM method.[39−43]

3.2. Equations. The regression error of the LSSVM[40] algorithm has been defined as the deviations between the calculated/estimated hydrate dissociation pressure values (outputs) and the experimental ones (reported in Table 1),[5,9,47−55] which has been treated as an addition to the constraint of the optimization (minimization) problem. In the traditional SVM method,[39] the value of the regression error is normally optimized during the computational steps, while in the LSSVM algorithm,[40] the error is mathematically defined.[39−41,43]

The cost function of the used mathematical strategy[40] can be determined by the following equation:[39−41,43]

$$Q_{\mathrm{LSSVM}} = \frac{1}{2} w^T w + \gamma \sum_{k=1}^{N} e_k^2 \tag{4}$$

subjected to the following constraint:

$$y_k = w^T \varphi(x_k) + b + e_k \quad k = 1, 2, \ldots, N \tag{5}$$

In the two preceding equations, x_k stands for the input vector containing the input elements of the model (temperature and pore size); y_k is the output vector (dependent parameter), b denotes the intercept of the linear regression in the LSSVM method;[40] w stands for the regression weight (slope of the linear regression); φ is the feature map, mapping the feasible region (input space) to a high dimensional feature space, in which the experimental hydrate dissociation data can be linearly separable by a hyperplane; e_k is the regression error for N training objects (the least-squares error approach); γ indicates the relative weight of the summation of the regression errors compared to the regression weight (first right-hand side of eq 4); and superscript T denotes the transpose matrix.

The regression weight (w) can be written as follows:[39−41,43]

$$w = \sum_{k=1}^{N} \alpha_k x_k \tag{6}$$

where

$$\alpha_k = 2\gamma e_k \tag{7}$$

Assuming the linear regression between the independent and the dependent variables of the LSSVM algorithm,[40] eq 5 is rewritten as:[39−41,43]

$$y = \sum_{k=1}^{N} \alpha_k {x_k}^T x + b \tag{8}$$

where x is the value of x_k when k is equal to 1. Therefore, the Lagrange multipliers in eq 4 are calculated as:[39−41,43]

$$\alpha_k = \frac{(y_k - b)}{{x_k}^T x + (2\gamma)^{-1}} \tag{9}$$

The preceding linear regression can be well converted to nonlinear one using the Kernel function as follows:[39−41,43]

$$f(x) = \sum_{k=1}^{N} \alpha_k K(x, x_k) + b \tag{10}$$

where $K(x, x_k)$ is the Kernel function calculated from the inner product of the two vectors x and x_k in the feasible region built by the inner product of the vectors $\Phi(x)$ and $\Phi(x_k)$ as follows:[39−41,43]

$$K(x, x_k) = \Phi(x)^T \cdot \Phi(x_k) \tag{11}$$

In this work, the radial basis function (RBF) Kernel has been applied, which is indicated by the following expression:[39−41,43]

$$K(x, x_k) = \exp(-||x_k - x||^2/\sigma^2) \tag{12}$$

where σ is considered to be a decision variable, which is treated by an external optimization algorithm during the internal LSSVM[40] calculations. The mean square error (MSE) of the

Table 2. Optimum Values of the LSSVM[40] Models Parameters for Different Systems

hydrate former	porous media	γ	σ^2
CH_4	silica gel	1000	1.167
CH_4	mesoporous silica	10^6	1.000
CH_4	porous glass	10^6	54.266
CO_2	silica gel	23325	3.255
CO_2	porous glass	10^6	479.7
C_2H_6	silica gel	10^6	4.630

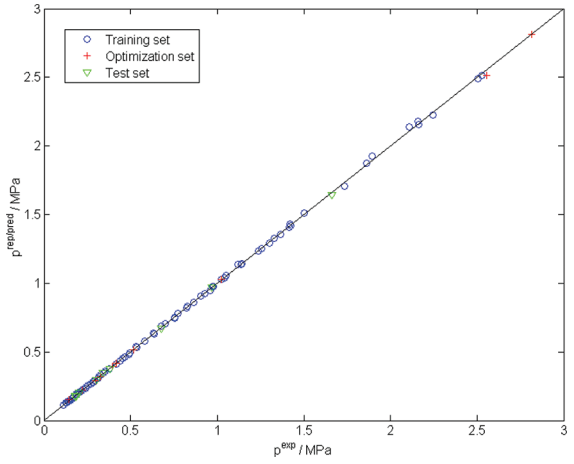

Figure 1. Comparison between the represented (rep) and the predicted (pred) ethane hydrate dissociation pressure values in the presence of silica gel porous media using the LSSVM[40] mathematical model and the corresponding experimental ones.[47,50]

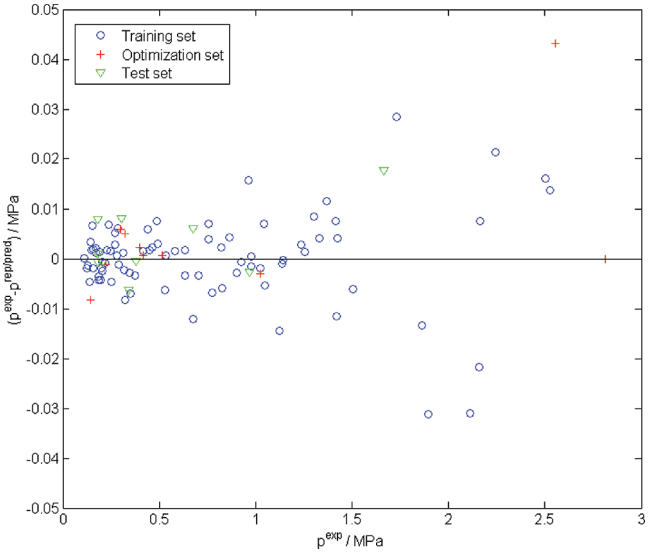

Figure 2. Deviations of the represented (rep)/predicted (pred) ethane hydrate dissociation pressure values in the presence of silica gel using the LSSVM[40] mathematical model from the experimental data.[47,50]

results of the LSSVM[40] algorithm has been defined as:

$$\mathrm{MSE} = \frac{\sum_{i=1}^{n} \left(p_{\mathrm{rep./pred.}\,i} - p_{\mathrm{exp.}\,i}\right)^2}{ns - nn} \qquad (13)$$

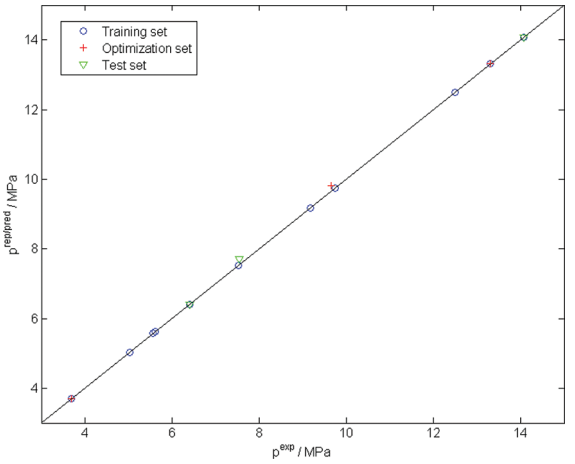

Figure 3. Comparison between the represented (rep) and the predicted (pred) methane hydrate dissociation pressure values in the presence of mesoporous silica media using the LSSVM[40] mathematical model and the corresponding experimental ones.[5,52]

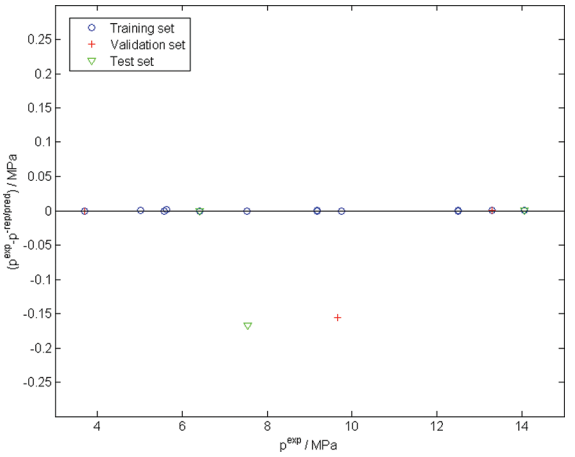

Figure 4. Deviations of the represented (rep)/predicted (pred) methane hydrate dissociation pressure values in the presence of mesoporous silica using the LSSVM[40] mathematical model from the experimental data.[5,52]

where p is the hydrate dissociation pressure, subscripts rep./pred. and exp. indicate the represented/predicted and experimental dissociation pressure values,[5,9,47−55] respectively, *ns* is the number of samples from the initial population, and *nn* denotes the number of model parameters. In this work, we have used the LSSVM[40] algorithm developed by Pelckmans et al.[41] and Suykens and Vandewalle[40] with modification of the optimization part that will be described later.

3.3. Computational Procedure. The hydrate dissociation pressure values have been normalized between −1 and +1 to prevent truncation errors. Moreover, this procedure, which is generally performed in optimization process, has been applied to obtain the parameters of the LSSVM[40] algorithm (γ and σ^2), and it has no effects on the model results. Later, these values are again changed to the original equilibrium pressures. In the next step, the experimental databases regarding the clathrate hydrates phase equilibria of each system are divided into three subdata sets including the "training" set, the

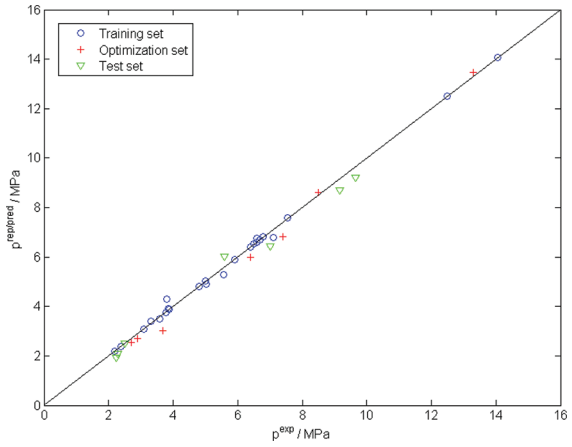

Figure 5. Comparison between the represented (rep) and the predicted (pred) methane hydrate dissociation pressure values in the presence of glass porous media using the LSSVM[40] mathematical model and the corresponding experimental ones.[53−55]

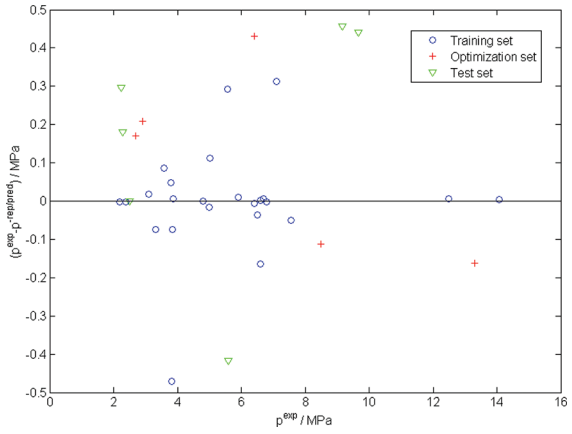

Figure 6. Deviations of the represented (rep)/predicted (pred) methane hydrate dissociation pressure values in the presence of porous glass media using the LSSVM[40] mathematical model from the experimental data.[53−55]

"optimization" set, and the "test" set. In this study, the "training" set is used to generate the model structure, the "optimization" set is applied for optimization of the model parameters, and the "test (prediction)" set is used to investigate the prediction capability and validity of the proposed model. The division of database into three subdata sets is normally performed randomly. For this purpose, about 80, 10, and 10% of the main data set are (randomly) selected for the "training" set, the "optimization" set, and the "test" set. The effect of the number of the data assigned to each subdata sets on the reliability of the final model results has been already discussed.[56] As for the distribution of the data through the three subdata sets, we normally conduct many distributions to avoid the local accumulations of the data in the feasible region of the problem. As a result, the acceptable distribution is the one with homogeneous accumulations of the data on the domain of the three subdata sets.[27−30,43,44]

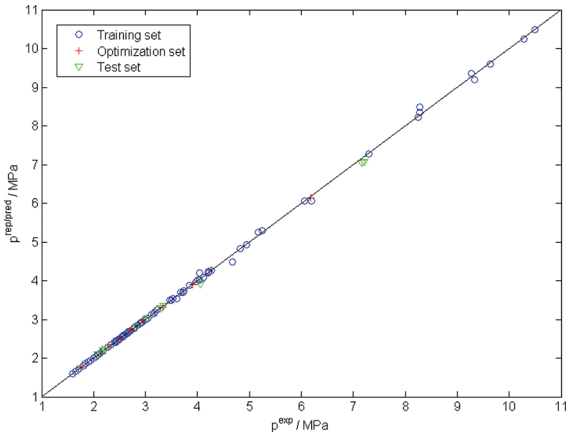

Figure 7. Comparison between the represented (rep) and the predicted (pred) methane hydrate dissociation pressure values in the presence of silica gel porous media using the LSSVM[40] mathematical model and the corresponding experimental ones.[9,47,48]

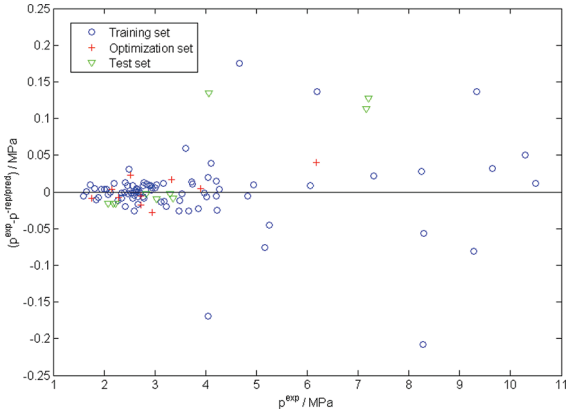

Figure 8. Deviations of the represented (rep)/predicted (pred) methane hydrate dissociation pressure values in the presence of silica gel porous media using the LSSVM[40] mathematical model from the experimental data.[9,47,48]

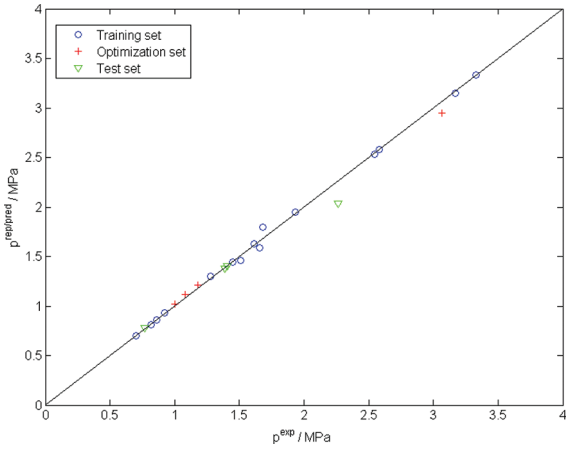

Figure 9. Comparison between the represented (rep) and the predicted (pred) carbon dioxide hydrate dissociation pressure values in the presence of porous glass media using the LSSVM[40] mathematical model and the corresponding experimental ones.[54,55]

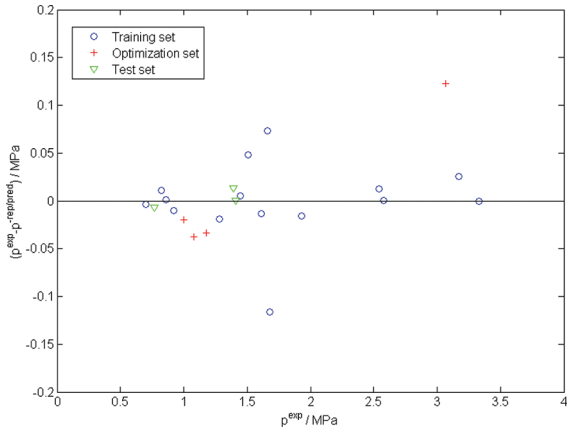

Figure 10. Deviations of the represented (rep)/predicted (pred) carbon dioxide hydrate dissociation pressure values in the presence of glass porous media using the LSSVM[40] mathematical model from the experimental data.[54,55]

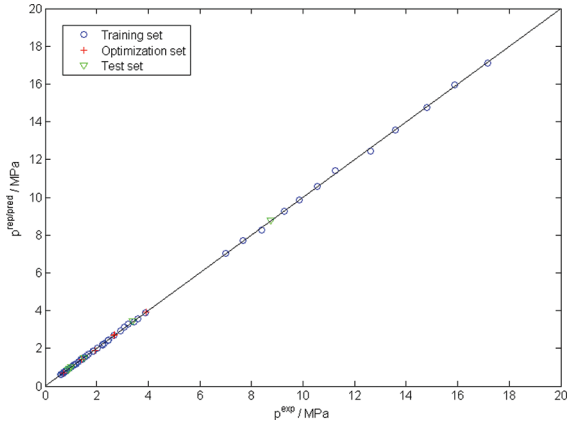

Figure 11. Comparison between the represented (rep) and the predicted (pred) carbon dioxide hydrate dissociation pressure values in the presence of silica gel porous media using the LSSVM[40] mathematical model and the corresponding experimental ones.[47,49]

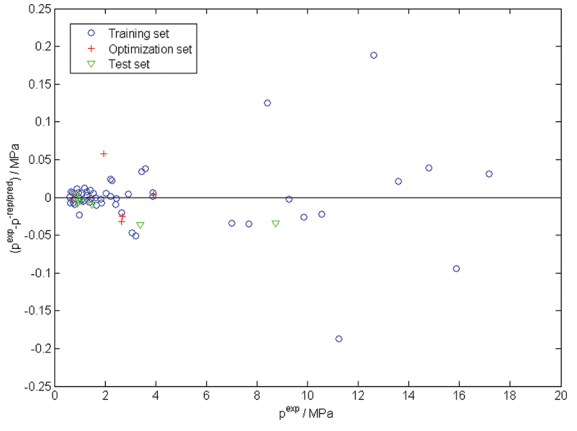

Figure 12. Deviations of the represented (rep)/predicted (pred) carbon dioxide hydrate dissociation pressure values in the presence of silica gel porous media using the LSSVM[40] mathematical model from the experimental data.[47,49]

Table 3. Statistical Parameters of the Developed LSSVM[40] Mathematical Model To Determine the Ethane Hydrate Dissociation Pressure Values in the Presence of Silica Gel Porous Media

statistical parameter	value
training set	
R^{2a}	1.000
average absolute relative deviation,[b] (%)	1.0
standard deviation error	0.009
root mean square error (MSE)	0.009
N^c	82
optimization set	
R^2	1.000
average absolute relative deviation	1.3
standard deviation error	0.014
root MSE	0.014
N	10
test set	
R^2	1.000
average absolute relative deviation	1.2
standard deviation error	0.007
root MSE	0.007
N	10
training + optimization + test set	
R^2	1.000
average absolute relative deviation	1.0
standard deviation error	0.009
root MSE	0.009
N	102

[a] Squared correlation coefficient. [b] % AARD = $(100/(N-n))\ \Sigma_i^N\{[|\text{Rep.}(i)/\text{Pred.}(i) - \text{Exp.}(i)|]/\text{Exp.}(i)\}$, where n is the number of the model parameters. [c] Number of experimental data.

4. RESULTS AND DISCUSSION

The experimental data investigated in this work are reviewed in Table 1. It was assumed that all of the studied porous media pores have cylindrical shape (based on the conditions reported in the original articles).

4.1. LSSVM[40] Models. The computational steps have been performed following the described procedure. The two main parameters of this algorithm are σ^2 and γ, which are supposed to be optimized using an appropriate optimization strategy. To select a suitable and efficient optimization algorithm, the characteristics of the corresponding method should be considered as follows:[43,57−67]

1. High capabilities to treat nondifferentiable, nonlinear, and multimodal cost functions;
2. No requirement of extensive problem formulation;
3. Few assumptions about the underlying objective functions;
4. Few control variables to pursue the minimization procedure;
5. No sensitivity to starting points;
6. No requirement of very detailed information about the structure of the problem space for definition of the objective function;

Table 4. Statistical Parameters of the Developed LSSVM[40] Mathematical Model To Determine the Methane Hydrate Dissociation Pressure Values in the Presence of Mesoporous Silica Media

statistical parameter	value
training set	
R^2	1.000
average absolute relative deviation (%)	0.0
standard deviation error	0.001
root MSE	0.001
N	14
optimization set	
R^2	1.000
average absolute relative deviation	0.5
standard deviation error	0.090
root MSE	0.090
N	3
test set	
R^2	1.000
average absolute relative deviation	0.7
standard deviation error	0.096
root MSE	0.096
N	3
training + optimization + test set	
R^2	1.000
average absolute relative deviation	0.2
standard deviation error	0.050
root MSE	0.051
N	20

Table 5. Statistical Parameters of the Developed LSSVM[40] Mathematical Model To Determine the Methane Hydrate Dissociation Pressure Values in the Presence of Porous Glass Media

statistical parameter	value
training set	
R^2	0.997
average absolute relative deviation (%)	1.6
standard deviation error	0.143
root MSE	0.140
N	24
optimization set	
R^2	0.995
average absolute relative deviation	7.0
standard deviation error	0.325
root MSE	0.395
N	7
test set	
R^2	0.990
average absolute relative deviation	6.6
standard deviation error	0.336
root MSE	0.379
N	7
training + optimization + test set	
R^2	0.993
average absolute relative deviation	3.5
standard deviation error	0.248
root MSE	0.260
N	38

7. Consistent convergence to the probable global optimum in consecutive independent trials.

Because of high nonlinearity of the SVM-based methods and the mentioned criteria, application of nonpopulation-based optimization methods such as simplex simulated annealing algorithm (M-SIMPSA)[68] or Levenberg−Marquardt (LM)[69,70] may be conservative for the current problem[43] (and perhaps for other problems on phase equilibria of such systems). In this work, we have modified the optimization part of the LSSVM[40] algorithm developed by Pelckmans et al.[41] and Suykens and Vandewalle[40] to use the robust genetic algorithm (GA) method.[37] This modification not only results in quicker computational steps but also solves the problem of sensitivity to starting points in conventional optimization techniques. Therefore, the optimization toolbox of MATLAB software has been employed, which is able to perform parallel computations. The number of populations of the optimization algorithm applied in this study has been set to 1000. To ensure that the value of the final solution is very close to the global optimum of the problem, the optimization procedure has been repeated several times.

The values of the probable global optima of the problems (although evaluation of the real global optima of the problems may not be generally simple); that is, a compromise between all of the local optima is reported in Table 2. It is worth it to point out that the numbers of the reported digits of these parameters are generally determined by sensitivity analysis of the total errors of the optimization procedure with respect to the corresponding values.

Figures 1−12 show the represented/predicted hydrate dissociation pressures applying the developed LSSVM models vs experimental values.[5,9,47−55] Tables 3−8 indicate the statistical parameters of the proposed models. Furthermore, the detailed determined hydrate dissociation conditions, experimental phase equilibrium data,[5,9,47−55] and the absolute relative deviations (ARD %) of results from experimental values[5,9,47−55] are reported in Tables 1−6 in the Supporting Information. The developed computer programs based on the proposed models and instructions for their method of running are freely available upon request to the authors. Therefore, anyone can easily apply the software to reproduce all of our results and predict phase equilibria of the investigated systems at temperature conditions of interest (in hydrate formation region).

It should be pointed out that our calculations show that the proposed LSSVM-based mathematical models do not contribute to reliable results for the phase equilibria of the propane clathrate hydrates in the presence of various porous media (not discussed in the current article). Another element to consider is that the average absolute relative deviations (AARD %) of the determined hydrate dissociation pressure values from the experimental ones are generally less than 3%. Therefore, we may not suspect any hydrate dissociation data point as the outliers of the developed mathematical models. Otherwise, it would have been fruitful to further check the reliability of the outliers by

Table 6. Statistical Parameters of the Developed LSSVM[40] Mathematical Model To Determine the Methane Hydrate Dissociation Pressure Values in the Presence of Silica Gel Porous Media

statistical parameter	value
training set	
R^2	1.000
average absolute relative deviation (%)	0.5
standard deviation error	0.046
root MSE	0.046
N	85
optimization set	
R^2	1.000
average absolute relative deviation	0.5
standard deviation error	0.020
root MSE	0.019
N	10
test set	
R^2	1.000
average absolute relative deviation	1.0
standard deviation error	0.066
root MSE	0.069
N	10
training + optimization + test set	
R^2	0.999
average absolute relative deviation	0.6
standard deviation error	0.047
root MSE	0.047
N	105

Table 7. Statistical Parameters of the Developed LSSVM[40] Mathematical Model To Determine the Carbon Dioxide Hydrate Dissociation Pressure Values in the Presence of Porous Glass Media

statistical parameter	value
training set	
R^2	0.998
average absolute relative deviation (%)	1.5
standard deviation error	0.041
root MSE	0.039
N	15
optimization set	
R^2	1.000
average absolute relative deviation	3.1
standard deviation error	0.077
root MSE	0.067
N	4
test set	
R^2	0.991
average absolute relative deviation	3.0
standard deviation error	0.112
root MSE	0.113
N	4
training + optimization + test set	
R^2	0.994
average absolute relative deviation	2.0
standard deviation error	0.064
root MSE	0.063
N	23

developing similar models excluding those points. Finally, any extrapolation of the developed mathematical models for other hydrate formers or porous media may not be recommended due to the fact that the models have been trained only on the carbon dioxide, methane, and ethane experimental hydrate phase equilibrium data in the presence of silica gel, mesoporous silica, and porous silica glass.

4.2. Proposed Correlation. The predictions of the applied correlation along with the existing experimental methane hydrate dissociation data in the presence of mesoporous silica glass reported in the literature are presented in Figure 13. The experimental IPD data ($\Delta T_{ice,pore}$) of Anderson et al.[55] have been used to check the reliability of prediction of eq 3. The clathrate hydrate dissociation temperatures at the bulk conditions are calculated from the thermodynamic model[71−73] previously proved to provide accurate results for the corresponding systems. In this model, general phase equilibrium criterion (equality of fugacities of each component throughout all phases present) has been used to perform the equilibrium calculations. For this purpose, the Valderrama modification of the Patel and Teja (VPT) equation of state (EoS)[74] accompanied with nondensity-dependent (NDD) mixing rules[75] has been applied to evaluate the fugacities of components in fluid phases, while the hydrate phase has been modeled using the van der Waals and Platteeuw (vdW-P) solid solution theory.[10] The details of this model have been already well-established.[71−73]

As can be seen, the agreement between the results of the correlation and the experimental data[55] are generally acceptable, demonstrating the reliability of eq 3 for predicting the changes in hydrate dissociation temperature at any given pressure due to the effect of pores from the corresponding changes in the ice point. Figure 14 similarly indicates the predicted carbon dioxide clathrate hydrate phase equilibria in the presence of mesoporous silica glass in comparison with the available experimental data.[55] Again, good coincidence between the predicted results and the experimental ones is observed. The represented/predicted of the developed LSSVM[40] models are also shown in the two preceding figures. It is obviously concluded that the represented/predicted methane or carbon dioxide hydrate dissociation pressures in the presence of silica glass porous media using the LSSVM models[40] is generally more accurate as compared with the predictions of the correlation (except the results for the hydrate phase equilibria of carbon dioxide in the porous media with pore size of 15 nm). It is worth pointing out that the corresponding thermodynamic models based on the vdW-P[10] theory and Gibbs−Thomson relationship reported in the literature generally lead to AARDs % between 2 and 9% for predictions of the CH_4 clathrate hydrate dissociation pressures and between 2 and 14% for those of CO_2 and C_2H_6 in the presence of silica gel porous media with different pore sizes.

In the final analysis, it should be noted that the applicability of the applied correlation is limited to those systems, for which the experimental IPD data ($\Delta T_{ice,pore}$) are available. Therefore, we

Table 8. Statistical Parameters of the Developed LSSVM[40] Mathematical Model To Determine the Carbon Dioxide Hydrate Dissociation Pressure Values in the Presence of Silica Gel Porous Media

statistical parameter	value
training set	
R^2	1.000
average absolute relative deviation (%)	0.6
standard deviation error	0.046
root MSE	0.046
N	54
optimization set	
R^2	0.999
average absolute relative deviation	0.9
standard deviation error	0.032
root MSE	0.029
N	6
test set	
R^2	1.000
average absolute relative deviation	0.7
standard deviation error	0.017
root MSE	0.021
N	6
training + optimization + test set	
R^2	1.000
average absolute relative deviation	0.7
standard deviation error	0.043
root MSE	0.043
N	66

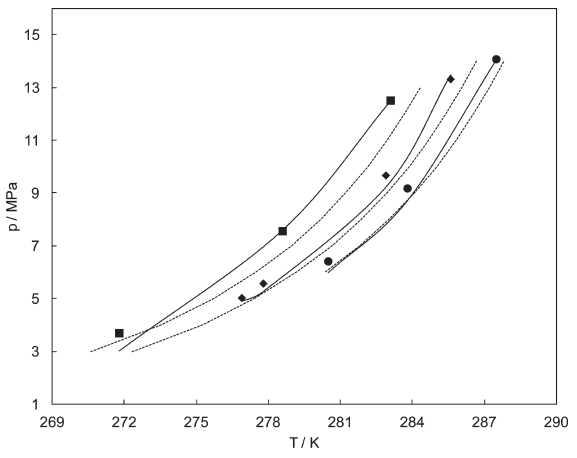

Figure 13. Experimental and predicted dissociation conditions of methane hydrates in the presence of silica glass porous media. Solid lines: Predictions of the developed LSSVM[40] models. Dashed lines: Predictions of the correlation (eq 3). Symbols: Experimental data [pore sizes: 9.2 (■), 15.8 (♦), and 30.6 nm (●)].[55]

are not able to check the capability of this correlation for all of the investigated systems treated using the developed mathematical LSSVM[40] models.

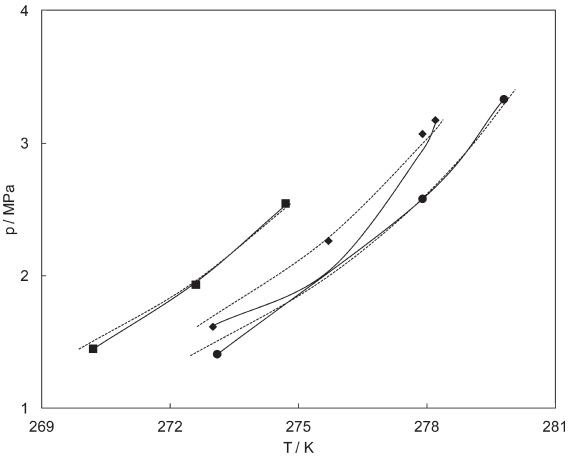

Figure 14. Experimental and predicted dissociation conditions of carbon dioxide hydrates in the presence of silica glass porous media. Solid lines: Predictions of the developed LSSVM[40] models. Dashed lines: Predictions of the correlation (eq 3). Symbols: Experimental data [pore sizes: 9.2 (■), 15.8 (♦), and 30.6 nm (●)].[55]

5. CONCLUSIONS

In this communication, we proposed two approaches for determination of the phase equilibria of clathrate hydrates of methane, carbon dioxide, and ethane in the presence of different kinds of porous media. A linear relationship between IPD of aqueous solution in porous media and hydrate dissociation temperature was implemented to provide a predictive correlation for this purpose. Furthermore, several mathematical models based on the least-squares SVM[40] were developed to represent/predict the corresponding hydrate dissociation conditions. It was found that the two proposed methods lead to generally acceptable agreement with the investigated experimental clathrate hydrate dissociation data from the literature,[5,9,47−55] although with some limitations. In spite of the fact that application of the reported correlation can significantly reduce the requirement of corresponding phase equilibrium data to tune the related thermodynamic models, its use is limited to the porous media, for which the experimental IPD data ($\Delta T_{ice,pore}$) are available (or at least can be estimated). In addition, it should be noted that the obtained LSSVM[40] mathematical models may not be able to predict the hydrate dissociation conditions of other systems excluding those investigated in this work, although they seem to be more general models than the applied correlation.

■ ASSOCIATED CONTENT

Ⓢ Supporting Information. Detailed determined hydrate dissociation conditions, experimental phase equilibrium data,[5,9,47−55] and the absolute relative deviations of results from experimental values. This material is available free of charge via the Internet at http://pubs.acs.org.

■ AUTHOR INFORMATION

Corresponding Author

*Tel: +(33)1 64 69 49 70. Fax: +(33)1 64 69 49 68. E-mail: amir-hossein.mohammadi@mines-paristech.fr.

■ ACKNOWLEDGMENT

A.E. is grateful to MINES ParisTech for providing him a Ph.D. scholarship.

■ REFERENCES

(1) Sloan, E. D.; Koh, C. A. *Clathrate Hydrates of Natural Gases*, 3rd ed.; CRC Press: New York, 2008.

(2) Chen, L. T.; Sun, C. Y.; Chen, G. J.; Nie, Y. Q. Thermodynamics model of predicting gas hydrate in porous media based on reaction-adsorption two-step formation mechanism. *Ind. Eng. Chem. Res.* **2010**, *49*, 3936–3943.

(3) Seo, Y.; Lee, S.; Cha, I.; Lee, J. D.; Lee, H. Phase equilibria and thermodynamic modeling of ethane and propane hydrates in porous silica gels. *J. Phys. Chem. B* **2009**, *113*, 5487–5492.

(4) Klauda, J. B.; Sandler, S. I. Predictions of gas hydrate phase equilibria and amounts in natural sediment porous media. *Mar. Pet. Geol.* **2003**, *20*, 459–470.

(5) Llamedo, M.; Anderson, R.; Tohidi, B. Thermodynamic prediction of clathrate hydrate dissociation conditions in mesoporous media. *Am. Mineral.* **2004**, *89*, 1264–1270.

(6) Clennell, M. B.; Hovland, M.; Booth, J. S.; Henry, P.; Winters, W. J. Formation of Natural Gas Hydrates in Marine Sediments: 1. Conceptual Model of Gas Hydrate Growth Conditioned by Host Sediment Properties. *J. Geophys. Res.* **1999**, *104*, 22985–23003.

(7) Brewer, P. G.; Orr, F. M.; Friederich, G.; Kvenvolden, K. A.; Orange, D. L. Gas hydrate formation in the deep sea: In situ experiments with controlled release of methane, natural gas, and carbon dioxide. *Energy Fuels* **1998**, *12*, 183–188.

(8) Eslamimanesh, A.; Mohammadi, A. H.; Richon, D.; Naidoo, P.; Ramjugernath, D. Application of gas hydrate formation in separation processes: A review of experimental studies. *J. Chem. Thermodyn.* **2012**, *46*, 62–71.

(9) Handa, Y. P.; Stupin, D. Thermodynamic properties and dissociation characteristics of methane and propane hydrates in 70-angstrom-radius silica-gel pores. *J. Phys. Chem.* **1992**, *96*, 8599–8603.

(10) van der Waals, J. H.; Platteeuw, J. C. Clathrate solutions. *Adv. Chem. Phys.* **1959**, *2*, 1–57.

(11) Eslamimanesh, A.; Mohammadi, A. H.; Richon, D. Thermodynamic model for predicting phase equilibria of simple clathrate hydrates of refrigerants. *Chem. Eng. Sci.* **2011**, *66*, 5439–5445.

(12) Tumba, K.; Reddy, P.; Naidoo, P.; Ramjugernath, D.; Eslamimanesh, A.; Mohammadi, A. H.; Richon, D. Phase equilibria of methane and carbon dioxide clathrate hydrates in the presence of aqueous solutions of tributylmethylphosphonium methylsulfate ionic liquid. *J. Chem. Eng. Data* **2011**, *56*, 3620–3629.

(13) Eslamimanesh, A.; Mohammadi, A. H.; Richon, D. Thermodynamic consistency test for experimental data of water content of methane. *AIChE J.* **2011**, *57*, 2566–2573.

(14) Eslamimanesh, A.; Mohammadi, A. H.; Richon, D. Thermodynamic consistency test for experimental solubility data in carbon dioxide/methane + water system inside and outside gas hydrate formation region. *J. Chem. Eng. Data* **2011**, *56*, 1573–1586.

(15) Clarke, M. A.; Pooladi-Darvish, M.; Bishnoi, P. R. A method to predict equilibrium conditions of gas hydrate formation in porous media. *Ind. Eng. Chem. Res.* **1999**, *38*, 2485–2490.

(16) Wilder, J. W.; Seshadri, K.; Smith, D. H. Modeling hydrate formation in media with broad pore size distributions. *Langmuir* **2001**, *17*, 6729–6735.

(17) Klauda, J. B.; Sandler, S. I. Modeling gas hydrate phase equilibria in laboratory and natural porous media. *Ind. Eng. Chem. Res.* **2001**, *40*, 4197–4208.

(18) Klauda, J. B.; Sandler, S. I. A fugacity model for gas hydrate phase equilibria. *Ind. Eng. Chem. Res.* **2000**, *39*, 3377–3386.

(19) Klauda, J. B.; Sandler, S. I. Predictions of gas hydrate phase equilibria and amounts in natural sediment porous media. *Mar. Pet. Geol.* **2003**, *20*, 459–470.

(20) Bhangale, A. Y.; Zhu, T.; McGrail, B. P.; White, M. D. A model to predict gas hydrate equilibrium and gas hydrate saturation in porous media including mixed CO_2-CH_4 hydrates, 15th SPE-DOE Improved Oil Recovery Symposium: Old Reservoirs New Tricks A Global Perspective, Tulsa, OK, 2006.

(21) Li, X. S.; Zhang, Y.; Li, G.; Chen, Z. Y.; Yan, K. F.; Li, Q. P. Gas hydrate equilibrium dissociation conditions in porous media using two thermodynamic approaches. *J. Chem. Thermodyn.* **2008**, *40*, 1464–1474.

(22) Chen, G. J.; Guo, T. M. Thermodynamic modeling of hydrate formation based on new concepts. *Fluid Phase Equilib.* **1996**, *122*, 43–65.

(23) Chen, G. J.; Guo, T. M. A new approach to gas hydrate modeling. *Chem. Eng. J.* **1998**, *71*, 145–151.

(24) Momeni, K.; Sadeghi, M. T.; Fanaei, M. A. Prediction of methane and ethane hydrate phase equilibria in porous media using artificial neural network. Proceedings of the Third International Conference on Modeling, Simulation and Applied Optimization Sharjah, U.A.E January 20−22, 2009.

(25) Najibi, H.; Mohammadi, A. H.; Tohidi, B. Estimating the hydrate safety margin in the presence of salt and/or organic inhibitor using freezing point depression data of aqueous solutions. *Ind. Eng. Chem. Res.* **2006**, *45*, 4441–4446.

(26) Mohammadi, A. H.; Richon, D. Useful Remarks to Reduce Experimental Information Required to Determine Gas Hydrate Inhibition Effects of Thermodynamic Inhibitors. In *Natural Gas Research Progress*; David, N., Michel, T., Eds.; Nova Science Publishers: New York, 2008; pp 417−465.

(27) Gharagheizi, F.; Eslamimanesh, A.; Mohammadi, A. H.; Richon, D. Handling a very large data set for determination of surface tension of chemical compounds: A quantitative structure-property relationship strategy. *Chem. Eng. Sci.* **2011**, *66*, 4991–5023.

(28) Gharagheizi, F.; Eslamimanesh, A.; Mohammadi, A. H.; Richon, D. Representation/prediction of solubilities of pure compounds in water using artificial neural network−group contribution method. *J. Chem. Eng. Data* **2011**, *56*, 720–726.

(29) Gharagheizi, F.; Eslamimanesh, A.; Mohammadi, A. H.; Richon, D. QSPR approach for determination of parachor of non-electrolyte organic compounds. *Chem. Eng. Sci.* **2011**, *66*, 2959–2967.

(30) Gharagheizi, F. New neural network group contribution model for estimation of lower flammability limit temperature of pure compounds. *Ind. Eng. Chem. Res.* **2009**, *48*, 7406–7416.

(31) Chouai, A.; Laugier, S.; Richon, D. Modeling of thermodynamic properties using neural networks: Application to refrigerants. *Fluid Phase Equilib.* **2002**, *199*, 53–62.

(32) Piazza, L.; Scalabrin, G.; Marchi, P.; Richon, D. Enhancement of the extended corresponding states techniques for thermodynamic modelling. I. Pure fluids. *Int. J. Refrig.* **2006**, *29*, 1182–1194.

(33) Scalabrin, G.; Marchi, P.; Bettio, L.; Richon, D. Enhancement of the extended corresponding states techniques for thermodynamic modelling. II. Mixtures. *Int. J. Refrig.* **2006**, *29*, 1195–1207.

(34) Chapoy, A.; Mohammadi, A. H.; Richon, D. Predicting the hydrate stability zones of natural gases using artificial neural networks. *Oil Gas Sci. Technol.—Rev. IFP* **2007**, *62*, 701–706.

(35) Eslamimanesh, A.; Gharagheizi, F.; Mohammadi, A. H.; Richon, D. Artificial neural network modeling of solubility of supercritical carbon dioxide in 24 commonly used ionic liquids. *Chem. Eng. Sci.* **2011**, *66*, 3039–3044.

(36) Gharagheizi, F.; Eslamimanesh, A.; Mohammadi, A. H.; Richon, D. Artificial neural network modeling of solubilities of 21 mostly-used industrial solid compounds in supercritical carbon dioxide. *Ind. Eng. Chem. Res.* **2011**, *50*, 221–226.

(37) Holland, J. H. *Adaptation in Natural and Artificial Systems*; University of Michigan Press: Ann Arbor, 1975.

(38) Hagan, M.; Demuth, H. B.; Beale, M. H. *Neural Network Design*; International Thomson Publishing: Boston, 2002.

(39) Suykens, J. A. K.; Van Gestel, T.; De Brabanter, J.; De Moor, B.; Vandewalle, J. *Least Squares Support Vector Machines*; World Scientific: Singapore, 2002.

(40) Suykens, J. A. K.; Vandewalle, J. Least squares support vector machine classifiers. *Neural Process. Lett.* **1999**, *9*, 293–300.
(41) Pelckmans, K.; Suykens, J. A. K.; Van Gestel, T.; De Brabanter, D.; Lukas, L.; Hamers, B.; De Moor, B.; Vandewalle, J. *LS-SVMlab: A Matlab/C Toolbox for Least Squares Support Vector Machines*; Internal Report 02-44, ESATSISTA; K. U. Leuven: Leuven, Belgium, 2002.
(42) Curilem, M.; Acuña, G.; Cubillos, F.; Vyhmeister, E. Neural networks and support vector machine models applied to energy consumption optimization in semiautogeneous grinding. *Chem. Eng. Trans.* **2011**, *25*, 761–766.
(43) Gharagheizi, F.; Eslamimanesh, A.; Farjood, F.; Mohammadi, A. H.; Richon, D. Solubility parameter of non-electrolyte organic compounds: Determination using quantitative structure property relationship strategy. *Ind. Eng. Chem. Res.* **2011**, *50*, 11382–11395.
(44) Gharagheizi, F.; Eslamimanesh, A.; Mohammadi, A. H.; Richon, D. Group contribution-based method for determination of solubility parameter of non-electrolyte organic compounds. *Ind. Eng. Chem. Res.* **2011**, *50*, 10344–10349.
(45) Liu, H.; Yao, X.; Zhang, R.; Liu, M.; Hu, Z.; Fan, B. Accurate quantitative structure-property relationship model to predict the solubility of C60 in various solvents based on a novel approach using a least-squares support vector machine. *J. Phys. Chem. B* **2005**, *109*, 20565–20571.
(46) Yao, X.; Liu, H.; Zhang, R.; Liu, M.; Hu, Z.; Panaye, A.; Doucet, J. P.; Fan, B. QSAR and classification study of 1,4-dihydropyridine calcium channel antagonists based on least squares support vector machines. *Mol. Pharmaceutics* **2005**, *5*, 348–356.
(47) Seo, Y.; Lee, H.; Tsutomu, U. Methane and carbon dioxide hydrate phase behavior in small porous silica gels: Three-phase equilibrium determination and thermodynamic modeling. *Langmuir* **2002**, *18*, 9164–9170.
(48) Smith, D. H.; Wilder, J. W; Seshadri, K. Methane hydrate equilibria in silica gels with broad pore- size distributions. *AIChE J.* **2002**, *48*, 393–400.
(49) Smith, D. H.; Wilder, J. W.; Seshadri, K. Thermodynamics of carbon dioxide hydrate formation in media with broad pore-size distributions. *Environ. Sci. Technol.* **2002**, *36*, 5192–5198.
(50) Zhang, W.; Wilder, J. W.; Smith, D. H. Interpretation of ethane hydrate equilibrium data for porous media involving hydrate-ice equilibria. *AIChE J.* **2002**, *48*, 2324–2331.
(51) Seo, Y.; Lee, S.; Cha, I.; Lee, J. D.; Lee, H. Phase equilibria and thermodynamic modeling of ethane and propane hydrates in porous silica gels. *J. Phys. Chem. B* **2009**, *113*, 5487–5492.
(52) Anderson, R.; Llamedo, M.; Tohidi, B.; Burgass, R. W. Characteristics of clathrate hydrate equilibria in mesopores and interpretation of experimental data. *J. Phys. Chem. B* **2003**, *107*, 3500–3506.
(53) Uchida, T.; Ebinuma, T.; Takeya, S.; Nagao, J.; Narita, H. Dissociation condition measurements of methane hydrate in confined small pores of porous glass. *J. Phys. Chem. B* **1999**, *103*, 3659–3662.
(54) Smith, D. H.; Seshadri, K.; Uchida, T.; Wilder, J. W. Thermodynamics of methane, propane, and carbon dioxide hydrates in porous glass. *AIChE J.* **2004**, *50*, 1589–1598.
(55) Anderson, R.; Llamedo, M.; Tohidi, B.; Burgass, R. W. Experimental measurement of methane and carbon dioxide clathrate hydrate equilibria in mesoporous silica. *J. Phys. Chem. B* **2003**, *107*, 3507–3514.
(56) Gharagheizi, F. QSPR analysis for intrinsic viscosity of polymer solutions by means of GA-MLR and RBFNN. *Comput. Mater. Sci.* **2007**, *40*, 159.
(57) Price, K.; Storn, R. Differential Evolution. *Dr. Dobb's J.* **1997**, *22*, 18–24.
(58) Weise, T. Global Optimization Algorithms, Theory and Application, 2nd ed.; Accessed July 2011.
(59) Chiou, J. P.; Wang, F. S. Hybrid method of evolutionary algorithms for static and dynamic optimization problems with applications to a fed-batch fermentation process. *Comput. Chem. Eng.* **1999**, *23*, 1277–1291.
(60) Schwefel, H. P. *Numerical Optimization of Computer Models*; John Wiley & Sons: New York, 1981.
(61) Goldberg, D. E. *Genetic Algorithms in Search, Optimization, and Machine Learning*; Addison-Wesley: Reading, MA, 1989.
(62) Davis, L. *Handbook of Genetic Algorithms*; Van Nostrand Reinhold: New York, 1991.
(63) Storn, R. Differential evolution—A simple and efficient heuristic for global optimization over continuous spaces. *J. Global Optim.* **1997**, *11*, 341–359.
(64) Eslamimanesh, A. A semicontinuous thermodynamic model for prediction of asphaltene precipitation in oil reservoirs. M.Sc. Thesis; Shiraz University: Shiraz, Iran, 2009 (in Persian).
(65) Eslamimanesh, A.; Shariati, A. A Semicontinuous thermodynamic model for prediction of asphaltene precipitation, Presented at VIII Iberoamerican Conference on Phase Equilibria and Fluid Properties for Process Design (Equifase), Praia da Rocha, Portugal, Oct. 2009.
(66) Eslamimanesh, A.; Esmaeilzadeh, F. Estimation of solubility parameter by the modified ER equation of state. *Fluid Phase Equilib.* **2010**, *291*, 141–150.
(67) Yazdizadeh, M.; Eslamimanesh, A.; Esmaeilzadeh, F. Thermodynamic modeling of solubilities of various solid compounds in supercritical carbon dioxide: Effects of equations of state and mixing rules. *J. Supercrit. Fluids* **2011**, *55*, 861–875.
(68) Cardoso, M. F.; Salcedo, R. L.; Feyo de Azevedo, S.; Barbosa, D. A simulated annealing approach to the solution of minlp problems. *Comput. Chem. Eng.* **1997**, *21*, 1349–1364.
(69) Levenberg, K. A method for the solution of certain problems in least squares. *Quart. Appl. Math.* **1944**, *2*, 164–168.
(70) Marquardt, D. An algorithm for least-squares estimations of non-linear parameters. *SIAM J. Appl. Math.* **1963**, 431–441.
(71) Avlonitis, D. Thermodynamics of gas hydrate equilibria. Ph.D. Thesis, Department of Petroleum Engineering, Heriot-Watt University: Edinburgh, United Kingdom, 1992.
(72) Tohidi-Kalorazi, B. Gas hydrate equilibria in the presence of electrolyte solutions. Ph.D. Thesis, Department of Petroleum Engineering, Heriot-Watt University: Edinburgh, United Kingdom, 1995.
(73) Mohammadi, A. H.; Anderson, R.; Tohidi, B. Carbon monoxide clathrate hydrates: Equilibrium data and thermodynamic modeling. *AIChE J.* **2005**, *51*, 2825–2833.
(74) Valderrama, J. O. A generalized Patel-Teja equation of state for polar and non-polar fluids and their mixtures. *J. Chem. Eng. Jpn.* **1990**, *23*, 87–91.
(75) Avlonitis, D.; Danesh, A.; Todd, A. C. Prediction of VL and VLL equilibria of mixtures containing petroleum reservoir fluids and methanol with a cubic EoS. *Fluid Phase Equilib.* **1994**, *94*, 181–216.